Methods for assessing the epistemic uncertainty captured in ground-motion models

Guillermo Aldama Bustos
Jacobs Engineering UK Limited: Jacobs UK Limited
John Douglas (john.douglas@strath.ac.uk)
University of Strathclyde https://orcid.org/0000-0003-3822-0060
Fleur Strasser
Jacobs Engineering UK Limited: Jacobs UK Limited
Manuela Daví
Jacobs Engineering UK Limited: Jacobs UK Limited
Alice MacGregor
EDF Energy

Research Article

Keywords: seismic hazard, ground-motion model, epistemic uncertainty, backbone model, nuclear, United Kingdom (UK)

Posted Date: May 26th, 2022

DOI: https://doi.org/10.21203/rs.3.rs-1661512/v1

Abstract

A key task when developing a ground-motion model (GMM) is to demonstrate that it captures an appropriate level of epistemic uncertainty. This is true whether multiple ground motion prediction equations (GMPEs) are used or a backbone approach is followed. The GMM developed for a seismic hazard assessment for the site of a UK new-build nuclear power plant is used as an example to discuss complementary approaches to assess epistemic uncertainty. Firstly, trellis plots showing the various percentiles of the GMM are examined for relevant magnitudes, distances and structural periods to search for evidence of "pinching", where the percentiles narrow excessively. Secondly, Sammon's maps, including GMPEs that were excluded from the logic tree, are examined to check the spread of the GMPEs for relevant magnitudes and distances in a single plot. Thirdly, contour plots of the standard deviation of the logarithms of predicted ground motions from each branch of the logic tree (σ_μ) are compared with plots drawn for other relevant hazard studies. Fourthly, uncertainties implied by a backbone GMM derived using the Campbell (2003)'s hybrid stochastic empirical method are compared to those of the proposed multi-GMPE GMM. Finally, the spread of the percentile of hazard curves resulting from implementing the GMM are examined for different return periods to check whether any bands of lower uncertainty in ground-motion space resulted in bands of lower uncertainty in hazard space. These five approaches enabled a systematic assessment of the level of uncertainty captured by the proposed GMM.

1 Introduction

Probabilistic seismic hazard assessments (PSHAs) for sites of critical infrastructure (e.g. nuclear power plants) comprise two principal components. The first component is a seismic-source model (SSM) capturing forecasts of the future earthquakes (in terms of their locations, magnitudes and other characteristics) that could generate strong ground motions of engineering significance. The second component is a ground-motion model (GMM) providing estimates of the median and distribution of strong ground motions for each of the earthquakes in the seismic-source model for intensity measures (IMs) that are useful for the design or assessment of the infrastructure. Both of these models are associated with considerable epistemic uncertainty because of a lack of knowledge and data (e.g. incomplete earthquake catalogues, a lack of local strong-motion data and sparse measurements of geotechnical and geophysical characteristics) from the region surrounding the site and from the site itself. The reader is referred to the recent landmark article on this topic by Bommer (2022).

It has often been shown (e.g. Bradley et al. 2012; Pecker et al. 2017; Porter et al. 2012) that the epistemic uncertainty in the GMM is one of, if not *the*, largest contributor to the uncertainties in the final hazard results. Consequently, within seismic hazard assessments there are often considerable efforts made in measuring, comparing and justifying the levels of epistemic uncertainty captured in the GMM. The methods to undertake these steps and the basis of these judgements are not commonly presented in international peer-reviewed journals but are often only contained within reports of commercial projects. The purpose of this article, therefore, is, firstly, to describe work undertaken within a recent PSHA for the site of a new-build nuclear power plant in the UK, Sizewell C (SZC), to assess the epistemic uncertainty in

the ground-motion model developed for this project and, secondly, to summarise the arguments used to judge the level of uncertainty captured.

The PSHA for the SZC site was conducted using an approach similar to that followed for the PSHA for the Hinkley Point C site and described by Aldama-Bustos et al. (2019) and Tromans et al. (2019). This approach, which aimed to satisfy UK nuclear regulatory requirements, emphasised: technical rigour, use of modern data and techniques, expert elicitation, logical treatment of uncertainties and review and oversight by means of a three-member external peer review team (PRT). One of the main focusses of the PRT was that the epistemic uncertainties at all stages of the PSHA were being sufficiently well captured in terms of the centre, body and range (CBR) of the technical defensible interpretations (USNRC 2018). In particular, the PRT expressed interest in whether “pinching” (i.e. when predictions from all, or a significant number of, alternative models in the logic tree converge to a single value, or narrow excessively, at a particular magnitude-distance-period scenario) is present in the GMM proposed for this project and what impact this has on the overall uncertainty in the hazard results. The work presented in this article was undertaken partly because of this request from the PRT.

In the next section the GMM developed using the multi-ground motion prediction equation (GMPE) approach to predict the median PGA and elastic response pseudo-spectral accelerations (PSAs), the principal IMs of interest for the client, is described. The following section presents an alternative GMM developed using the backbone approach, which was compared to the proposed GMM. Sections 4, 5 and 6 describe three approaches (trellis plots, Sammon’s maps and σ_μ contour plots) used to investigate the epistemic uncertainty captured in the proposed GMM and compare it to uncertainties in GMMs from comparable projects. Section 7 shows how the ground-motion uncertainty transfers to uncertainty in the hazard results at the reference velocity horizon. The penultimate section discusses how these various pieces of evidence were used to judge the capturing of epistemic uncertainty within the GMM. The article ends with some brief conclusions.

2 Szc Ground-motion Model For Median

The development of the proposed SZC GMM followed what is commonly referred as the “traditional” or “multi-GMPE” approach. The selection of the suite of GMPEs considered in the GMM followed a rigorous and systematic approach where candidate models were identified using the comprehensive compendium of published GMPEs by Douglas (2018). The preliminary exclusion criteria were predominantly based on recommendations from Cotton et al. (2006) and Bommer et al. (2010), with consideration also given to selection criteria used in previous project for nuclear facilities (e.g. Renault 2014). From this preliminary selection, 11 GMPEs were retained for further assessment. These GMPEs were assessed by comparing ground-motion predictions from each of the individual GMPEs for various earthquake scenarios in terms of distance and magnitude scaling and in terms of response spectra. Also, Sammon’s maps were produced for selected IMs considering the magnitude and distance ranges of interest to the PSHA; this allowed identifying clusters of GMPEs in ground-motion space.

The assessment process was complemented by comparing predictions to various observations of ground shaking from a project-specific database that included ground-motion records from the UK, northern France, Belgium and western Germany. Comparisons against ground-shaking observations, although important and necessary, provided only limited, qualitative, guidance for the selection of the most appropriate GMPEs for a site-specific PSHA in the UK. This was mainly because of the small number of records available, which are limited to those from events with magnitudes generally below **M** 5.3 recorded at considerably (> 100 km) source-to-site distances. Also, due to limitations of the instrumental data (e.g. a lack of detailed site information for most strong-motion stations), quantitative methods to assess the match between predictions from the GMPEs and observations, such as those proposed by Scherbaum et al. (2004, 2009), were not applied.

The final step of the GMPE selection process consisted of an expert assessment of the preliminary selected GMPEs by the GMM team based on the comparisons previously described. The aim of this assessment was to reduce the number of candidate GMPEs to a more manageable figure, whilst ensuring that the range of selected GMPEs was sufficient to account for the considerable epistemic uncertainty associated with ground-motion prediction in the UK. Other factors, such as whether the GMPEs could be adjusted for site-specific conditions or would allow scaling to correct for stress drop variation were also taken into consideration, along with other technical and project-specific issues.

As result of this process, the following suite of GMPEs were selected for the proposed GMM:

- Bindi et al. (2014a; b) [BETAL14] – model using R_{JB} and V_{S30}
- Cauzzi et al. (2015) [CETAL15] – considering the period dependent reference V_{S30} option
- Chiou and Youngs (2014) [CY14]
- Rietbrock and Edwards (2019) [RE19] – 5 MPa stress-drop model
- Yenier and Atkinson (2015) [YA15] – model for central and eastern North America (CENA)

The compatibility of the ground-motion predictions from the selected suite of GMPEs was reviewed as the GMPEs may use different definitions of the predicted ground motion parameters and explanatory variables. The only compatibility issue identified was the consideration of alternative faulting mechanisms or “style of faulting”. BETAL14, CETAL15 and CY14 all include a style-of-faulting term in their functional from; also, the criterion used to define style-of-faulting is consistent across these three models. However, RE19 and YA15 do not provide an explicit style-of-faulting.

To address the style-of-faulting compatibility issue, reverse to strike-slip and normal to strike-slip adjustment factors ($F_{RV/SS}$ and $F_{N/SS}$, respectively) were developed. Predictions from the YA15 model were adjusted using these adjustment factors, following the approach recommended by Bommer et al. (2003), in conjunction with the faulting composition observed in the NGA East flatfile (i.e. 68% reverse, 2% normal and 30% strike-slip). Predictions from the RE19 model were left unadjusted as any adjustments required were estimated to be small (< 1%). Therefore, any improvements in the predictions are likely to be

offset by the introduction of additional epistemic uncertainty in the development of the adjustment factors.

All selected GMPEs are generic (i.e. non-site specific) models based on data from regions other than the UK, with exception of RE19 which used UK data. Therefore, the GMPEs required adjustments to consider the site-specific conditions at the reference velocity horizon, which for this study was defined at 82 m depth, with a V_{S30} of 1,139 m/s. These adjustments were performed via the application of host-to-target adjustments (HTTAs) designed to account for differences in the shear-wave velocity profile, V_S, and the factor characterising the high-frequency attenuation, kappa. HTTAs are also commonly known as V_S-kappa adjustments.

The calculation of the HTTAs requires four inputs to be defined, the average V_S profiles of the host ($V_{S,host}$) and target ($V_{S,target}$) locations, which allow the amplification due to V_S impedance to be computed; and the average kappa in the host ($kappa_{host}$) and target ($kappa_{target}$) locations, which allow for modelling differences in the high-frequency attenuation.

The $V_{S,host}$ profiles were assessed based on the information provided by the model developers for the stochastic models (RE19 and YA15). For the three empirical models (BETAL14, CETAL15 and CY14) the generic V_S profiles of Cotton et al. (2006) for a V_{S30} value of 1,000 m/s were used.

The $kappa_{host}$ values were assessed using the inverse random vibration theory technique (Al Atik et al. 2014) and considering a single pair of magnitude and distance (**M** 5.5 and 24 km) that are representative of the earthquake scenario controlling the hazard in the high-frequency range. The $kappa_{host}$ values assessed for the five selected GMPEs were: BETAL14, 0.0405 s; CETAL15, 0.0281 s; CY14, 0.0332 s; RE19, 0.0222 s; and YA15, 0.0209 s. These values are comparable to other estimates published for the same or similar GMPEs, where available (Zandieh et al. 2016).

The $V_{S,target}$ profile was developed based on the Poggi et al. (2011) V_S profile with a V_S of 1,100 m/s (V_{S30} of 1,139 m/s) at 82 m depth and 3,410 m/s at 4 km depth, which provided the best fit to site-specific data at the reference velocity horizon and the generic UK model (Turbitt 1985) and other regional deep V_S profiles (Davis et al. 2012; Ottemöller et al. 2009) at around 4 km.

The best estimate $kappa_{target}$ value for the site was thoroughly investigated for the project site using a combination of approaches including site-specific estimates from an “analogous” site (~ 70 km from the project site) with very similar geological conditions at the reference velocity horizon, estimates from other UK data/sites and estimates based on the V_{S30}-kappa correlations from global data. Based on these various estimates of kappa, the following logic-tree branches were used to construct the HTTAs: lower target kappa of 0.01 s; middle target kappa of 0.02 s; and higher target kappa of 0.03 s.

The approach of Al Atik et al. (2014) was extended to account for differences in V_S profiles as followed by Bommer et al. (2015) and Rodriguez-Marek et al. (2014), and then was implemented for the estimation

and application of the final HTTAs. The final HTTAs were developed for the three target kappa values stated above and all five GMPEs, leading to a suite of 15 adjustment factors.

Specifications for the SZC PSHA required the GMM should provide ground-motion for periods up to 10 s. To account for unrealistic behaviour observed in the predicted spectral displacements (SD) above T_D (i.e., the period at which the displacement spectrum becomes constant) and to extrapolate to periods above the longest period for which the GMPEs provide coefficients, the GMM team developed an approach to adjust long-period ground predictions for all GMPEs. This approach consisted of capping the SD for long periods at T_D, where T_D was calculated using the equation below assuming a stress drop, $\Delta\sigma$, of 80 bars (8 MPa):

$$Log_{10}(T_D) = -1.884 - \frac{Log_{10}(\Delta\sigma_{bars})}{3} + 0.5\boldsymbol{M} \qquad \text{Equation 1}$$

In the case where T_D was longer than the longest period for which the GMPE provides coefficients, a linear extrapolation was performed in the PSA domain considering a log-log scale for periods below T_D and capped at T_D, in the SD domain, for longer periods. T_D from the Equation 1 was constrained to be always above 1.0 s, where the predictions from the GMPEs are expected to be reliable and no adjustment is required.

The median ground-motion logic tree is presented in Figure 1. This captures the uncertainty in the selection of the most appropriate GMPE for the purposes of seismic hazard assessment at the SZC site as well as on the $kappa_{target}$. The weights assigned to the GMPEs were based on the assessments of the GMPE's merits and weaknesses and reflect the level of confidence in each particular GMPE to provide an appropriate prediction of the ground-motion amplitudes expected at the SZC site. Weights assigned to each $kappa_{target}$ branch reflect the GMM team's expectations, based on the assessment discussed above, that the "true" kappa value at the SZC site is more likely to be somewhere between 0.01 s and 0.02 s (and closer to the latter) than above 0.02 s.

3 Comparison To A Backbone Model

An alternative, which has been increasingly used in site-specific PSHAs, to using multiple GMPEs with V_S-kappa adjustments is the so-called "backbone" approach (e.g. Atkinson et al. 2014; Douglas 2018b). Therefore, one method that was used to judge the appropriateness of the epistemic uncertainty in the SZC GMM was to compare it to a UK backbone model that was developed specifically for this project. The backbone model presented in this section accounts for uncertainty in the median stress drop and the kappa at the bedrock horizon of the SZC site. It is noted that this backbone model is not recommended for use within PSHAs but as a point of reference to help assess whether the SZC multi-GMPE GMM is capturing the CBR of the expected ground motions at the SZC site.

3.1 Application of the hybrid-empirical method for the SZC site

In their recent article Bommer and Stafford (2020) recommend using the Chiou and Youngs (2014) GMPE as an empirical backbone GMPE for site-specific PSHAs. They propose branching out this backbone GMPE to capture uncertainty in the source, path and site conditions in the target region (in this case the region of the SZC site) using the hybrid empirical method (HEM) of Campbell (2003, 2004). The HEM adjusts an empirical GMPE [here, the Chiou and Youngs (2014)] for the host region [here, western North America, WNA, i.e. the host region of Chiou and Youngs (2014)] by multiplying predictions from this GMPE for each magnitude and distance of interest by the ratio between predictions from stochastic ground-motion models for the target region (here, the SZC site) and the host region (here, WNA) for that magnitude and distance. The output of this calculation is an “empirical” ground-motion model for the target region that accounts for effects (e.g. finite-fault behaviour) that cannot easily be accounted for by a stochastic model.

The HEM is useful for areas with little strong-motion data from which to derive fully empirical GMPEs as it provides a way to account, in a transparent manner, for uncertainties in the input parameters of the stochastic model for the target region. This is achieved by using alternative values for the various input parameters to the stochastic model along with weights expressing ‘belief’ in those values being appropriate for the target region. In this manner multiple target stochastic models are generated for each magnitude and distance each with appropriate overall weights. The latter are produced by multiplying the weights of each input parameter (correlations between input parameters can be modelled by only allowing certain combinations, although in the implementation presented here all combinations of parameters are allowed).

The HEM was used by Campbell (2003, 2004) to develop GMPEs for central and eastern North America (CENA) by adjusting GMPEs derived for WNA by multiplication by the ratio between stochastic models for CENA and WNA. Douglas et al. (2006), as part of a study to derive sets of GMPEs for southern Spain and southern Norway, developed an open-source Fortran program CHEEP[4] based on the SMSIM software[5] of David M. Boore to undertake the HEM. This program extends the HEM to account for uncertainties in the host stochastic model (because it is generally not possible to find a stochastic model that provides a perfect match to predictions from the empirical GMPE for the host region) as well as to convert the distance metrics of the empirical GMPEs and make other conversions of independent (e.g. style of faulting) and dependent parameters (e.g. horizontal component definitions). CHEEP was used to develop a preliminary backbone GMM for the SZC site.

3.1.1 Host stochastic model for Chiou and Youngs (2014)

Chiou and Youngs (2014) was not originally included within CHEEP as this software was developed about a decade before the Chiou and Youngs (2014) GMPE was published. As part of the SZC project a

new subroutine was included in CHEEP to evaluate the Chiou and Youngs (2014) GMPE. The HEM relies on having available a [in the original formulation of Campbell (2003, 2004)], or a set of [in the extended formulation of Douglas et al. (2006)], stochastic model(s) for the host region that closely fit(s) the empirical GMPE. CHEEP includes sets of 100 stochastic models for each of the 10 host empirical GMPEs that were coded in the original version of this software. These stochastic models were taken from Scherbaum et al. (2006), who used genetic algorithm search to determine the 100 best-fitting models for each GMPE to account for the uncertainty in the inversion process. CHEEP did not include Chiou and Youngs (2014) as one of its in-built GMPEs so stochastic models for this GMPE are also not available in the form required by this software. Because the software to repeat Scherbaum et al. (2006)'s inversion process is not available, the stochastic models provided in CHEEP for the WNA GMPEs of Abrahamson and Silva (1997) and Boore et al. (1997) were both used as proxies for the unavailable stochastic models for Chiou and Youngs (2014) and similar backbone GMMs obtained. By examining the match between the predictions from these stochastic models and the Chiou and Youngs (2014) GMPE over a wide range of magnitudes and distances it was confirmed that these stochastic models are suitable for the HEM. This is especially the case as the backbone GMM was only being used for comparisons and not for the actual PSHA, and because small misfits between empirical and stochastic host models have previously been shown to be relatively unimportant (Campbell 2003; Douglas et al. 2006).

3.1.2 Target stochastic model for SZC site

For the target stochastic models Table 2 of Rietbrock and Edwards (2019) was used for: source spectral shape, source duration, median stress drop parameter ($\Delta\sigma$=5, 10 and 20 MPa), geometric spreading, path attenuation Q (only the top layer of their layered structure was used because CHEEP cannot account for a layered Q structure – this simplification will have only a minor effect and mainly at large distances) and path duration (corrected for the two typographical errors that seem to be present in the publication of Rietbrock and Edwards (2019) for longer distances). This part of the stochastic model accounts for uncertainty in the median stress drop for the UK. The site amplification and attenuation components of the target stochastic models are the SZC shear-wave velocity profile and the three values of kappa proposed for this site (0.01, 0.02 and 0.03 s), which are discussed above. In total, there are $3 \times 3=9$ separate target stochastic models accounting for uncertainty in $\Delta\sigma$ and kappa.

3.1.3 Resulting backbone GMM

Running CHEEP for the inputs presented above leads to many thousands of samples of the median predicted ground motions for the 9 combinations of stress drop and kappa for all magnitudes (4 to 7.5 in steps of 0.25) and distances (from 1 to 300 km in roughly logarithmic steps) considered. Because of the use of multiple stochastic models for the host region and the conversion of distances metrics (Scherbaum et al., 2004) from rupture distance (for Chiou and Youngs 2014) to hypocentral distance (to

evaluate the stochastic models) to distance to the surface projection of rupture (for comparison with the other GMPEs for SZC) 100 Monte Carlo samples were required to obtain stable estimates of the ground motions at each magnitude and distance.

To facilitate the use of the models the samples for each magnitude and distance and given Δσ and kappa were averaged and then regression analysis conducted to obtain coefficients that can be used to evaluate the nine models for any magnitude and distance. The functional form assumed was that used by Campbell (2003) for his HEM for eastern North America (and also used by Douglas et al. (2006) for Norway) but modified to account for the distances at which the geometric spreading of Rietbrock and Edwards (2019) changes (50 km and 100 km). A check confirmed that this step introduced only a very minimal error [similar findings were reported by Douglas et al. (2006)]. The resulting backbone GMM is presented in Figure 2 with respect to distance for magnitude 5 and PGA. Results for other magnitudes and spectral periods show similar behaviour. The spread in the curves decreases as period increases as stress drop and kappa uncertainty in the target stochastic models only have a large influence at short structural periods.

Footnote:

[4] https://pureportal.strath.ac.uk/en/datasets/cheep-composite-hybrid-equation-estimation-program
[5] http://www.daveboore.com/software_online.html

4 Trellis Plots

To assess whether the predictions from the various GMPEs in the proposed SZC GMM narrow excessively at any particular magnitude-distance-period scenario, trellis plots were produced in terms of response spectra and distance scaling of the GMM predictions. These plots were drawn for percentiles between 0 and 100, in steps of 1 percent, for a number of selected IMs and for magnitudes between **M** 4.0 and 7.5, and distances between 0.1 and 100 km.

Median predictions of the Chiou and Youngs (2014) model, including the HTTA for the middle kappa (CY14-middle kappa), were also included in the response spectra and distance scaling plots. The main reason for this was to assess whether the SZC GMM is “well centred” based on the comparisons between the SZC GMM median predictions and the median predictions from a well-constrained model (i.e. CY14) adjusted to the local conditions at the SZC site. The CY14 model was selected for this comparison as it is suggested by Bommer and Stafford (2020) to be a good backbone model candidate. Distance scaling plots for PGA and PSA at 0.05, 0.2 and 1.0 s are presented in Fig. 3, while response spectra plots for **M** 4.0, 5.0, 6.0 and 7.0 are shown in Fig. 4.

In addition to the plots described above, distance attenuation and response spectra were produced comparing the 16th, 50th and 84th percentile predictions of the SZC GMM and the UK backbone model (see Section 3), for the same magnitudes, distances and periods previously described. These

comparisons are presented in Fig. 5 in terms of distance scaling and in Fig. 6 in terms of response spectra.

From these comparisons it was concluded that although “bands of lower epistemic uncertainty” (i.e. where the spread of the percentiles is reduced) were observed at specific periods and magnitude-distance ranges (e.g. the narrow spread of the percentiles observed in the response spectra for **M** 5.0 at 0.2 s in Fig. 4), these were not as excessively narrow so as to reject the GMM. These bands of lower uncertainty are more easily observed in the σ_μ plots presented in Section 6 and their effects on the uncertainty in the hazard space (i.e., at the reference velocity horizon) are discussed in Section 7.

SZC GMM median predictions are in good agreement with median predictions from the CY14-middle kappa model at distances shorter than ~ 80 km. At longer distances differences are driven mainly by the plateau on the attenuation of the ground motion at about 100 km, which is characteristic of stable continental regions (SCRs) and is not modelled by the CY14-middle kappa branch. In addition, there is generally a good agreement between the SZC GMM and UK backbone model predictions for the 16th, 50th and 84th percentiles. Again, differences at about 100 km are mainly due to the 50–100 km plateau assumed in the functional form of the target stochastic model, which is associated with Moho bounce effects and is characteristic of SCRs. However, as in the case of the RE19 model (from where the target stochastic model was taken), it is questionable whether these effects should be visible for > **M** 6 earthquakes where a significant part of the crust is ruptured.

In summary, comparisons between median predictions from SZC GMM and the CY14-middle kappa, and SZC GMM and UK backbone, provided confidence that the SZC GMM is well “centred”. Likewise, similarities in the distribution of the percentiles (16th, 50th and 84th) from the SZC GMM and the UK backbone suggest that the “body” of the epistemic uncertainty is also well captured by the SZC GMM.

5 Sammon’s Maps

As discussed in Section 2, Sammon’s maps were produced as part of the assessment and selection of the GMPEs comprising the SZC GMM. The Sammon’s map approach is based on a visualisation technique developed by Frank Scherbaum and co-workers (Scherbaum et al. 2010; Scherbaum and Kuehn 2011). The method has been implemented in various recent PSHA projects for nuclear facilities (e.g. PEGASOS Refinement Project, Thyspunt PSHA and NGA-East) to check the closeness of different GMPEs in ground-motion space. Such assessment helps ensure that epistemic uncertainty is adequately captured, whilst avoiding involuntary biases in the ground-motion distribution implied by the GMM logic tree. Such biases result from the fact that available GMPEs are frequently not independent from each other, as they are developed from overlapping, and in some cases, identical, databases.

Sammon’s maps were produced considering all GMPEs preliminary selected, which were considered sufficient for the purposes of this study to identify clustering of models or outliers. Figure 7 presents Sammon’s maps for PGA and PSA at 0.2 and 1.0 s. All preliminary GMPEs not included in the final GMM

are greyed out while the edges of the selected unadjusted GMPEs (i.e., without HTTAs) are colour coded; asterisks correspond to the 15 branches of the SZC GMM logic tree (i.e., HTTA-adjusted GMPEs) and the SZC GMM (i.e., weighted median prediction of the GMM logic tree) is shown as a red square. Note that Fig. 7 also includes rejected variants of the same GMPE, when provided by the developers of the GMPE (e.g. RE19 provides coefficients for stress drops of 5, 10 and 20 MPa; all three alternatives are plotted but only RE19-5MPa is colour coded).

The spread of the models in the two-dimensional surface can be considered representative of the range of the epistemic uncertainty in the ground-motion prediction captured by the models used in the analysis. This spread does not necessarily, and most likely does not, represent the full range of the epistemic uncertainty, which by definition is unknown. However, if a relatively large number of models, for relevant tectonic regimes, are included in the analysis, one could expect them to capture a range of epistemic uncertainty large enough as to be considered a reasonable (i.e., as close to the full range as possible) representation of the full range. This is the same principle behind the multi-GMPE approach.

From Fig. 7 it is observed that the 15 branches of the SZC GMM logic tree comfortably cover the ground-motion space indicated by all preliminary selected models, while the median predictions of the SZC GMM tends towards the centre. Also worth noting that no clustering of the 15 branches of the SZC GMM logic tree is observed. This confirms that the SZC GMM spans a range of behaviours in ground-motion space and suggests that the GMM is sufficiently diverse to capture epistemic uncertainty, whilst avoiding model redundancy.

6 σμ Plots

One way of judging if the level of epistemic uncertainty captured in the median ground-motion logic tree is appropriate is to compare it to the levels of uncertainty captured by other GMMs, particularly those developed for use in site-specific PSHA for critical infrastructure. A standard method of measuring the epistemic uncertainty is the standard deviation of the weighted natural logarithms of the estimates of the median ground motion (σ_{μ}, where μ is the natural logarithm of the estimates of the median ground motion), where the weights correspond to the weights assigned to the alternative models in the logic tree. It could be argued that the use of σ_{μ} is not ideal when considering a multi-GMPE GMM, as this measure is not directly captured in the PSHA (unlike when using some backbone models). We believe, however, that it is still a useful tool for comparison with other GMMs in the absence of a better alternative.

σ_{μ} plots were produced for a number of selected periods, for the SZC GMM and the ground-motion models listed below, with the objective of assessing the level of epistemic uncertainty captured by the SZC GMM (i.e. the “range” of the epistemic uncertainty):

- Preliminary UK backbone model developed (see Section 3);
- NGA-W2 models (Al Atik and Youngs 2013, 2014);
- NGA-East models (Goulet et al. 2018);

- SERA backbone model (Weatherill and Cotton 2020) - model for shallow seismicity in Europe;
- Wylfa PSHA (Villani et al. 2020) - multi-GMPE model for a NPP site in the UK; and
- Thyspunt PSHA (Bommer et al. 2015) - backbone GMM for a NPP site in South Africa.

The preliminary UK backbone model was developed as part of this study (see Section 3) with the purpose of developing a model that explicitly captured uncertainty in the source and site conditions in the target region (in this case the SZC site) using the HEM of Campbell (2003, 2004). This is used as a reference point to help assess whether the SZC GMM adequately captures the CBR of the expected ground motions at the SZC site.

Al Atik and Youngs (2013, 2014) assess the level of epistemic uncertainty captured by the set of NGA-W2 models (i.e. model-to-model variability) and propose a minimum additional epistemic uncertainty to lead to a more appropriate level of epistemic uncertainty. The minimum epistemic uncertainty suggested by Al Atik and Youngs (2014) for the NGA-W2 models captures the epistemic uncertainty in ground-motion estimation for active shallow crustal regions (ASCR), using the most complete and verified ground-motion database available worldwide. It could, therefore, be considered as a lower bound of epistemic uncertainty for GMMs in other regions (i.e. epistemic uncertainty in any other region can be expected to be higher).

The NGA-East GMPEs were developed specifically for CENA, using a range of alternative approaches for modelling ground motions in a region with scarce data (Goulet et al. 2018). The final suite of GMPEs was developed based on stochastic sampling using Sammon's maps of the GMPE space covered by the set of 'seed' GMPEs developed by the various modelling teams. The area in ground-motion space covered by the resampled models was considered to be representative of the epistemic uncertainty. This area was then divided into 17 sectors and a representative non-parametric model (i.e. a set of Magnitude-Distance-Frequency-lnY quadruplets, where lnY is the logarithmic ground-motion amplitude) selected for each sector. Weights for each of the 17 final models were then determined from comparisons of the model predictions with a subset of well-recorded data, considering both the fit to the data and the shape of the overall ground-motion distribution. The NGA-East models cover a very large study region where some of the parameters controlling ground-motion amplitudes (e.g. stress drop or crustal attenuation, Q) can be considered non-homogeneous, with regional adjustments only partially capturing the associated epistemic uncertainty. Therefore, the σ_μ values based on the weighted model-to-model variance of the 17 models developed as part of the NGA-East project, can be considered an upper bound of the modelling epistemic uncertainty (i.e. epistemic uncertainty in smaller regions with more homogeneous conditions can reasonably be expected to be lower).

Weatherill and Cotton (2020) developed a backbone model, referred herein as the SERA model, for shallow seismicity in Europe using the Kotha et al. (2020) GMPE as its backbone. This model was developed as part of the Horizon 2020 Seismology and Earthquake Engineering Research Infrastructure Alliance for Europe (SERA) project.

The ground-motion models developed for the Wylfa (Villani et al. 2020) and Thyspunt (Bommer et al. 2015) PSHAs were considered for comparisons with the SZC GMM as examples of what the UK nuclear regulator refers to as “relevant good practice” for single-site PSHAs. The Wylfa GMM is a site-specific, single-station, multi-GMPE model and consists of seven alternative GMPEs. Three of the seven GMPEs in this model are the alternative variants of the model by Rietbrock and Edwards (2019). As the Rietbrock and Edwards (2019) GMPEs were developed specifically for the UK, the authors of the Wylfa PSHA only applied HTTA factors to the GMPEs from other regions.

As part of the Thyspunt PSHA, the authors of the study developed a site-specific backbone model using the models of Akkar and Çağnan (2010), Abrahamson and Silva (2008) and Chiou and Youngs (2008) as the backbone GMPEs. This backbone model considered adjustment factors for V_S, kappa and stress drop parameters.

σ_μ plots were produced for a selected number of structural periods for each of the GMM discussed above and the proposed SZC GMM. Figure 8, Fig. 9 and Fig. 10 shows comparisons of the σ_μ estimates for all GMMs for PGA and PSA at 0.2 and 1.0 s, respectively, as examples. Note that, the Thyspunt GMM is not plotted for magnitudes below 5.0 because that PSHA used a minimum magnitude of 5, but the same magnitude scale on the horizontal axis was kept for easy comparison with the other GMMs.

From examination of the σ_μ plots across all selected structural periods, an epistemic uncertainty of ~ 0.2 could be considered as an acceptable lower bound, based on the uncertainty captured by the NGA-W2 models. In a similar manner, based on the uncertainty captured by the NGA East models, an upper bound for the epistemic uncertainty of ~ 0.4 could be defined for all structural periods, which could be increased up to ~ 0.5 for magnitudes higher than **M** 7.0. The uncertainty captured by the SZC GMM was generally above the lower bound of 0.2, with exception of structural periods above 1.0 s at very short distances (< 10 km) and a narrow band of magnitudes and distances (~ **M** 4.5 at 8 km) for periods around 0.5 s. However, this was considered not to affect significantly the epistemic uncertainty in hazard space at the reference velocity horizon, as discussed in the following section.

At the shorter structural periods, epistemic uncertainty in the SZC GMM was equivalent to the uncertainty in the UK backbone model and comparable with other models, including the NGA-East models. At intermediate periods (0.2–0.5 s) zones of lower epistemic uncertainty were observed in the SZC GMM. However, this seems to be a characteristic consistent across most of the selected GMMs (see NGA-W2, Thyspunt and Wylfa in Fig. 9), the only exception being the two backbone models that are based on a single GMPE (i.e. UK backbone and SERA). The reason for these zones of lower uncertainty is not clear. The presence of this feature in the total epistemic uncertainty recommended by Al Atik and Youngs (2013, 2014) for the NGA-W2 may suggest that these zones of lower uncertainty represent a real behaviour of the distribution of the epistemic uncertainty in the magnitude-distance space and across periods. This could be as a result of the presence of a larger number of good quality records for that range of period-magnitude-distance in the various databases used to derive the GMPEs, or simply that the variability at intermediate periods from variations in stress drop, geometric spreading, site amplification and other

characteristics is intrinsically lower. If these zones of lower uncertainty are a real feature of the epistemic uncertainty across response periods, it could be suggested that backbone models based on a single GMPE may fail to capture such features and overestimate the epistemic uncertainty at middle periods and at magnitude-distance scenarios that are likely to be relevant to the seismic hazard.

At long periods (≥ 1.0 s) the epistemic uncertainty captured by the SZC GMM is generally higher than in other models and is in good agreement with the NGA-East model. The exception is the Wylfa GMM, where epistemic uncertainty ranges between 0.5 and 1.0 for the range of magnitudes and distances expected to control the hazard. This is likely to be driven by unrealistic predictions at long periods from the RE19 models, particularly for the 10 and 20 MPa variants of this GMPE.

It is also worth noting the lack of magnitude dependency of the epistemic uncertainty in the SERA backbone and the very weak, almost null, distance dependency of the epistemic uncertainty in the UK backbone for periods above 0.2 s (at shorter periods the uncertainty is effectively uniform across all magnitudes and distances). This lack of magnitude or distance dependency could be argued to be an unrealistic distribution of the epistemic uncertainty as it is in disagreement with the epistemic uncertainty observed from physics-based models (Frankel 2018) where the epistemic uncertainty is magnitude and distance dependent.

7 Effect On Hazard

To understand how the epistemic uncertainty in the SZC GMM propagates to the hazard estimates at the reference velocity horizon, the Toro (2006) equation, as re-arranged by Douglas (2018b), was used to estimate σ_μ for the range of return periods and response periods relevant to the SZC PSHA (Fig. 11). These estimates were obtained using the hazard curves from the final hazard calculations of the SZC PSHA. This is especially important given the zones of lower epistemic uncertainty discussed in previous sections.

The re-arranged Toro (2006) equation uses the mean and median hazard curves from the hazard calculations to estimate σ_μ. There is currently no approach to split the epistemic uncertainty into the SSM and GMM parts from the hazard results (which accounts for the combined uncertainties in both the SSM and the GMM). σ_μ estimates obtained using the re-arranged Toro (2006) equation have, however, been observed to be a good approximation to the true uncertainty in the GMM (Douglas 2018c; Douglas et al. 2014).

The main difference between σ_μ values shown in Fig. 11 and σ_μ values in Fig. 8 to Fig. 10 is that σ_μ values in Fig. 11 directly account for the relative contributions to the total hazard of the range of magnitudes and distances considered in the SZC PSHA. As observed in Fig. 11, uncertainty in the hazard estimates tends to be lower at structural periods around 0.2 s, but remains, across all structural periods, consistently above the lower bound value of 0.2 defined as the lower acceptable value for the epistemic uncertainty from the GMM. As expected, the lower levels of uncertainty observed in the SZC GMM for

periods above 1.0 s, at short distances (< 10 km), do not have any significant contribution to the epistemic uncertainty at the reference velocity horizon where the observed σ_μ values are about 0.3 or higher.

8 Discussion

From observation of the trellis and σ_μ plots “bands of lower epistemic uncertainty” were identified at specific periods and magnitude-distance ranges. This issue is mitigated, however, by the hazard at the reference velocity horizon not being dominated by a single magnitude-distance scenario at any response period. This issue could become important if the hazard is controlled by magnitude-distance scenarios that correspond to those where lower epistemic uncertainty is observed.

Comparisons with the median predictions of the CY14-middle kappa, and selected percentiles of the UK backbone model, provided confidence that the SZC GMM is well “centred” and that it adequately captures the “body” of the epistemic uncertainty of the ground-motions expected at the SZC site. Also, from the distribution of the predictions from the 15 branches comprising the SZC GMM logic tree in the ground-motion space, as shown in the Sammon’s maps (Fig. 7), it can be considered that the SZC GMM adequately captures the “range” of the epistemic uncertainty while avoiding model redundancy.

In addition to this, the epistemic uncertainty captured by the SZC GMM, expressed in terms of σ_μ, is generally above the acceptable lower bound of 0.2, which was defined based on the uncertainty captured by the NGA-W2. The exception to this were periods above 1 s at very short distances (< 10 km) and a narrow band of magnitudes and distances (around **M** 4.5 at 8 km) for periods around 0.5 s. However, σ_μ estimates obtained using the re-arranged Toro (2006) equation (Fig. 11) confirmed that these lower bands of epistemic uncertainty only propagate slightly to the hazard estimates at the reference velocity horizon. These findings provided confidence that the epistemic uncertainty in the SZC GMM, for the magnitude-distance ranges of interest for the SZC PSHA, is sufficiently well captured.

One of the most significant challenges when assessing whether the level of epistemic uncertainty may be appropriate is the definition of a minimum level of uncertainty that could be considered adequate, or acceptable, at a given structural period and magnitude-distance range. In this study, this minimum level of uncertainty was defined as 0.2 based on the epistemic uncertainty captured by the NGA-W2 models. Comparisons against the variability observed from ground-motion measurements could also help to this end. In areas of low to very low seismicity levels, as is the case of the UK, the limitations of the available instrumental database (i.e., small magnitude events, typically below the lower magnitude of interest for PSHA, at long distances, > 100 km) do not allow a meaningful assessment of the ground-motion uncertainty. However, such assessments could be carried out using macroseismic intensity data, which in the case of the UK is relatively abundant and cover magnitude and distance scenarios relevant to PSHA (although there is still a lack for earthquakes with **M** > 5.5). This type of comparisons was not considered in the present assessment but may be useful in future studies.

9 Conclusion

Seismic hazard assessments are always associated with considerable epistemic uncertainty because of a lack of knowledge and information on potential future earthquakes in the region of the site and the strong ground motions that such events could generate. Capturing epistemic uncertainty within the seismic-source and ground-motion models of these assessments is critical, as is demonstrating to reviewers, the regulator and the client that the uncertainties are appropriate and well justified. This article has applied five methods to assess the epistemic uncertainty within the ground-motion model developed within a recent seismic hazard assessment for the site of a new-build nuclear power plant in the UK. In addition, the impact of uncertainties in the ground-motion model on the uncertainties in the hazard curves is also measured. Examining the results from applying these methods and comparing them to results for ground-motion models developed in comparable projects led the project team to conclude that the epistemic uncertainties were sufficiently well captured. This conclusion was also informed by how the epistemic uncertainty in the ground-motion model propagated to the reference velocity horizon, which is the key output of the hazard assessment.

Declarations

Acknowledgements

We thank the peer review team (PRT) of the SZC project, Drs Hilmar Bungum, Martin Koller and Zoe Shipton, for their detailed and constructive comments throughout this project.

Funding

We express our gratitude to SZC NNB GenCo, the sponsor of the project, for agreeing to the publication of this article.

Competing interests

The authors have no relevant financial or non-financial interests to disclose.

Author Contributions

All authors contributed to the study conception and design. Analyses were performed by Guillermo Aldama Bustos, John Douglas, Fleur Strasser and Manuela Daví. The first draft of the manuscript was written by Guillermo Aldama Bustos and John Douglas and all authors commented on previous versions of the manuscript. All authors read and approved the final manuscript.

Data availability

No data were used in the writing of this article.

References

1. Abrahamson NA, Silva WJ (1997) Empirical response spectral attenuation relations for shallow crustal earthquakes. Seismol Res Lett 68(1):94–127
2. Abrahamson N, Silva W (2008) Summary of the Abrahamson & Silva NGA ground-motion relations. Earthq Spectra 24(1):67–97
3. Akkar S, Çağnan Z (2010) A local ground-motion predictive model for Turkey, and its comparison with other regional and global ground-motion models. Bull Seismol Soc Am 100(6):2978–2995
4. Al Atik L, Kottke A, Abrahamson N, Hollenback J (2014) Kappa (κ) Scaling of ground-motion prediction equations using an inverse random vibration theory approach. Bull Seismol Soc Am 104(1):336–346
5. Al Atik L, Youngs RR (2013) *Epistemic uncertainty for NGA-West2 models*. PEER 2013/11. Pacific Earthquake Engineering Research Center, p 86
6. Al Atik L, Youngs RR (2014) Epistemic uncertainty for NGA-West2 models. Earthq Spectra 30(3):1301–1318
7. Aldama-Bustos G, Tromans IJ, Strasser FO, Garrard G, Green G, Rivers L, Douglas J, Musson RMW, Hunt S, Lessi-Cheimariou A, Daví M, Robertson C (2019) An innovative approach for the seismic hazard assessment of safety-significant facilities with high level of regulatory assurance requirements. Bull Earthq Eng 17(1):37–54
8. Atkinson GM, Bommer JJ, Abrahamson NA (2014) Alternative approaches to modeling epistemic uncertainty in ground motions in probabilistic seismic-hazard analysis. Seismol Res Lett 85(6):1141–1144
9. Bindi D, Massa M, Luzi L, Ameri G, Pacor F, Puglia R, Augliera P (2014a) Pan-European ground-motion prediction equations for the average horizontal component of PGA, PGV, and 5%-damped PSA at spectral periods up to 3.0 s using the RESORCE dataset. Bull Earthq Eng 12(1):391–430
10. Bindi D, Massa M, Luzi L, Ameri G, Pacor F, Puglia R, Augliera P (2014b) Erratum to: Pan-European ground-motion prediction equations for the average horizontal component of PGA, PGV, and 5%-damped PSA at spectral periods up to 3.0 s using the RESORCE dataset. Bull Earthq Eng 12(1):431–448
11. Bommer JJ (2022) Earthquake hazard and risk analysis for natural and induced seismicity: towards objective assessments in the face of uncertainty. Bull Earthq Eng 20(6):2825–3069
12. Bommer JJ, Coppersmith KJ, Coppersmith RT, Hanson KL, Mangongolo A, Neveling J, Rathje EM, Rodriguez-Marek A, Scherbaum F, Shelembe R (2015) and others. “A SSHAC level 3 probabilistic seismic hazard analysis for a new-build nuclear site in South Africa.” *Earthquake Spectra*, 31(2), 661–698
13. Bommer JJ, Douglas J, Scherbaum F, Cotton F, Bungum H, Fäh D (2010) On the selection of ground-motion prediction equations for seismic hazard analysis. Seismol Res Lett 81(5):783–793

14. Bommer JJ, Douglas J, Strasser FO (2003) Style-of-faulting in ground-motion prediction equations. Bull Earthq Eng 1(2):171–203
15. Bommer JJ, Stafford PJ (2020) Selecting ground-motion models for site-specific PSHA: adaptability versus applicability. Bull Seismol Soc Am 110(6):2801–2815
16. Boore DM, Joyner WB, Fumal TE (1997) Estimation of response spectra and peak accelerations from western North America earthquakes: A summary of recent work. Seismol Res Lett 68(1):128–153
17. Bradley BA, Stirling MW, McVerry GH, Gerstenberger M (2012) Consideration and propagation of epistemic uncertainties in New Zealand probabilistic seismic-hazard analysis. Bull Seismol Soc Am 102(4):1554–1568
18. Campbell KW (2003) Prediction of strong ground motion using the hybrid empirical method and its use in the development of ground-motion (attenuation) relations in Eastern North America. Bull Seismol Soc Am 93(3):1012–1033
19. Campbell KW (2004) Erratum to 'Prediction of strong ground motion using the hybrid empirical method and its use in the development of ground-motion (attenuation) relations in Eastern North America'. Bull Seismol Soc Am 94(6):2418
20. Cauzzi C, Faccioli E, Vanini M, Bianchini A (2015) Updated predictive equations for broadband (0.01–10 s) horizontal response spectra and peak ground motions, based on a global dataset of digital acceleration records. Bull Earthq Eng 13(6):1587–1612
21. Chiou BS-J, Youngs RR (2008) An NGA model for the average horizontal component of peak ground motion and response spectra. Earthq Spectra 24(1):173–215
22. Chiou BS-J, Youngs RR (2014) Update of the Chiou and Youngs NGA Model for the Average Horizontal Component of Peak Ground Motion and Response Spectra. Earthq Spectra 30(3):1117–1153
23. Cotton F, Scherbaum F, Bommer JJ, Bungum H (2006) Criteria for selecting and adjusting ground-motion models for specific target regions: Application to central Europe and rock sites. J Seismolog 10(2):137
24. Davis MW, White NJ, Priestley KF, Baptie BJ, Tilmann FJ (2012) Crustal structure of the British Isles and its epeirogenic consequences. Geophys J Int 190(2):705–725
25. Douglas J (2018a) "Ground motion prediction equations (1964–2018) by John Douglas, University of Strathclyde, Glasgow, United Kingdom." http://www.gmpe.org.uk/ (Aug. 29, 2018)
26. Douglas J (2018b) "Capturing geographically-varying uncertainty in earthquake ground motion models or what we think we know may change." *Recent Advances in Earthquake Engineering in Europe. ECEE 2018*, Geotechnical, Geological and Earthquake Engineering
27. Douglas J (2018c) "Calibrating the backbone approach for the development of earthquake ground motion models." Cadarache-Château, France, 11
28. Douglas J, Bungum H, Scherbaum F (2006) Ground-motion prediction equations for southern Spain and southern Norway obtained using the composite model perspective. J Earthq Eng Imperial Coll Press 10(01):33–72

29. Douglas J, Ulrich T, Bertil D, Rey J (2014) Comparison of the ranges of uncertainty captured in different seismic-hazard studies. Seismol Res Lett 85(5):977–985
30. Frankel A (2018) “Some concerns about the NGA-East GMM’s - or - Don’t forget about the science.” NSHM Workshop, 7 March 2018
31. Goulet CA, Bozorgnia Y, Abrahamson N, Kuehn N, Atik A, Youngs L, Graves R, Atkinson G (2018) *Central and eastern North America ground-motion characterization*. PEER Report No. 2018/08, Pacific Earthquake Engineering Research Center, Berkeley, California, 817 pgs
32. Kotha SR, Weatherill G, Bindi B, Cotton F (2020) A regionally-adaptable ground-motion model for shallow crustal earthquakes in Europe. Bull Earthq Eng 18:4091–4125
33. Ottemöller L, Baptie B, Smith NJP (2009) Source parameters for the 28 April 2007 Mw 4.0 earthquake in Folkestone, United Kingdom. Bull Seismol Soc Am 99(3):1853–1867
34. Pecker A, Faccioli E, Gurpinar A, Martin C, Renault P (2017) Seismic hazard computation. In: Geotechnical G, Engineering E, Pecker A, Faccioli E, Gurpinar A, Martin C (eds) ” An Overview of the SIGMA Research Project: A European Approach to Seismic Hazard Analysis. Springer International Publishing, Cham, pp 119–132
35. Poggi V, Edwards B, Fäh D (2011) Derivation of a reference shear-wave velocity model from empirical site amplification. Bull Seismol Soc Am 101(1):258–274
36. Porter KA, Field EH, Milner K (2012) Trimming the UCERF2 hazard logic tree. Seismol Res Lett 83(5):815–828
37. Renault P (2014) Approach and challenges for the seismic hazard assessment of nuclear power plants: the Swiss experience. Bolletino di Geofisica Teorica ed Applicata 55(5):149–164
38. Rietbrock A, Edwards B (2019) “Update of the UK stochastic ground motion model using a decade of broadband data.” *SECED 2019 Conference - Earthquake and engineering towards a resilient world*, Society for Earthquake and Civil Engineering Dynamics, Greenwich, London
39. Rodriguez-Marek A, Rathje EM, Bommer JJ, Scherbaum F, Stafford PJ (2014) Application of single-station sigma and site-response characterization in a probabilistic seismic-hazard analysis for a new nuclear site. Bull Seismol Soc Am 104(4):1601–1619
40. Scherbaum F, Cotton F, Smit P (2004a) On the use of response spectral reference data for the selection and ranking of ground motion models for seismic hazard analysis in regions of moderate seismicity: The case of rock motion. Bull Seismol Soc Am 94(6):2164–2185
41. Scherbaum F, Cotton F, Staedtke H (2006) The estimation of minimum-misfit stochastic models from empirical ground-motion prediction equations. Bull Seismol Soc Am 96(2):427–445
42. Scherbaum F, Delavaud E, Riggelsen C (2009) Model selection in seismic hazard analysis: an information-theoretic perspective. Bull Seismol Soc Am 99(6):3234–3247
43. Scherbaum F, Kuehn N (2011) Logic tree branch weights and probabilities: Summing up to one is not enough. Earthq Spectra 27(4):1237–1251

44. Scherbaum F, Kuehn NM, Ohrnberger M, Koehler A (2010) Exploring the proximity of ground-motion models using high-dimensional visualization techniques. Earthq Spectra 26(4):1117–1138
45. Scherbaum F, Schmedes J, Cotton F (2004b) On the conversion of source-to-site distance measures for extended earthquake source models. Bull Seismol Soc Am 94(3):1053–1069
46. Toro G (2006) “The effects of ground-motion uncertainty on seismic hazard results: Examples and approximate results.” Poster presented at the 2006 SSA Annual Meeting, San Francisco, California, USA
47. Tromans IJ, Aldama-Bustos G, Douglas J, Lessi-Cheimariou A, Hunt S, Daví M, Musson RMW, Garrard G, Strasser FO, Robertson C (2019) Probabilistic seismic hazard assessment for a new-built nuclear power plant in the UK. Bull Earthq Eng 17(1):1–36
48. Turbitt T (1985) *Catalogue of British earthquakes recorded by the BGS seismograph network 1982, 1983, 1984*. British Geological Survey, 52
49. USNRC (2018) Updated implementation guidelines for SSHAC hazard studies. NUREG-2213, p 145
50. Villani M, Lubkowski Z, Free M, Musson RMW, Polidoro B, McCully R, Koskosidi A, Oakman C, Courtney T, Walsh M (2020) A probabilistic seismic hazard assessment for Wylfa Newydd, a new nuclear site in the United Kingdom. Bull Earthq Eng 18(9):4061–4089
51. Weatherill G, Cotton F (2020) “A ground motion logic tree for seismic hazard analysis in the stable cratonic region of Europe: regionalisation, model selection and development of a scaled backbone approach.” *Bulletin of Earthquake Engineering*
52. Yenier E, Atkinson GM (2015) Regionally adjustable generic ground-motion prediction equation based on equivalent point-source simulations: Application to central and eastern North America. Bull Seismol Soc Am 105(4):1989–2009
53. Zandieh A, Campbell KW, Pezeshk S (2016) Estimation of κ0 Implied by the High-Frequency Shape of the NGA-West2 Ground-Motion Prediction Equations. Bull Seismol Soc Am 106(3):1342–1356
54. Statements and declarations

Figures

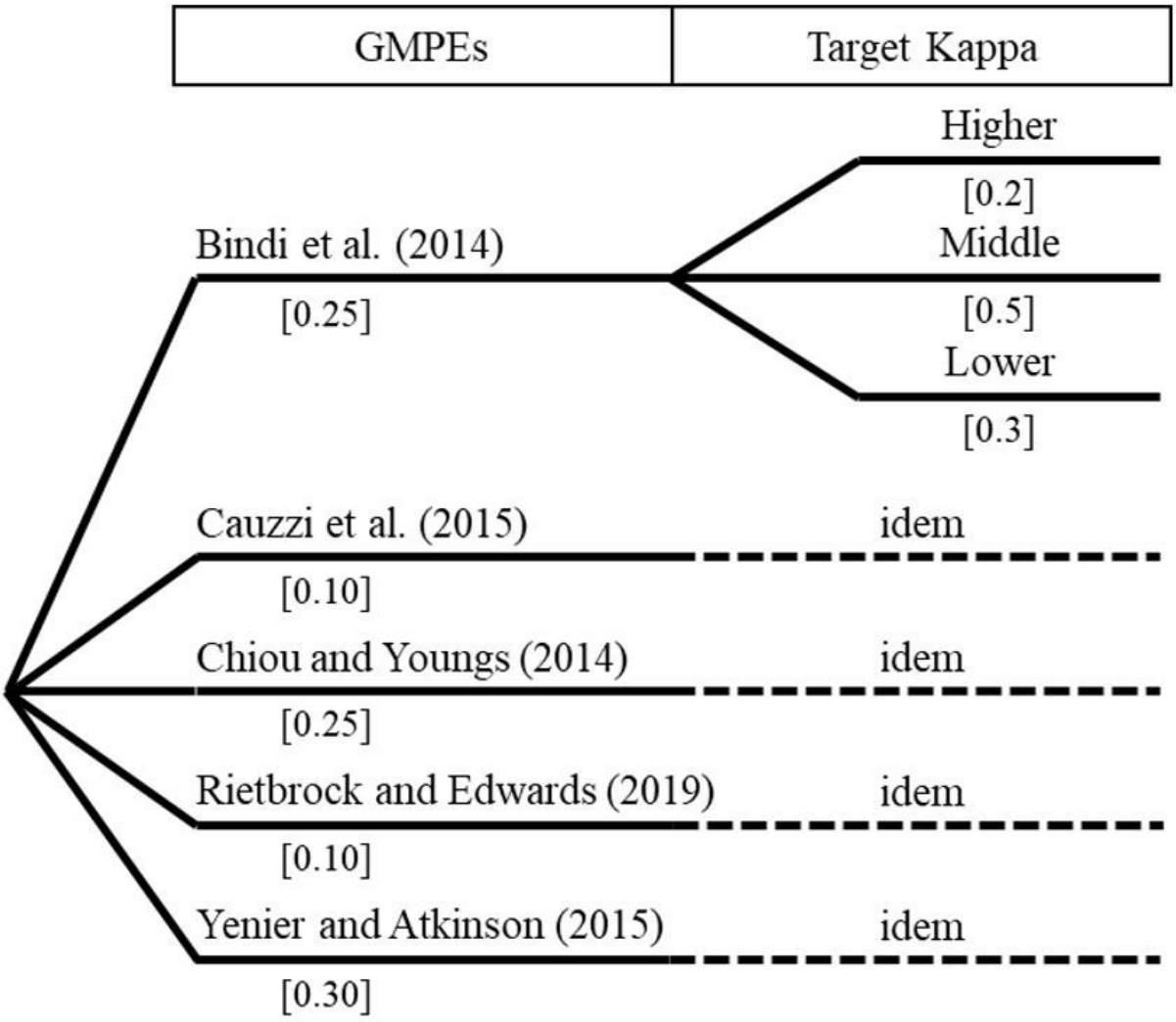

Figure 1

Median ground-motion logic tree for the SZC PSHA.

Numbers in square brackets are the weights assigned to each alternative branch.

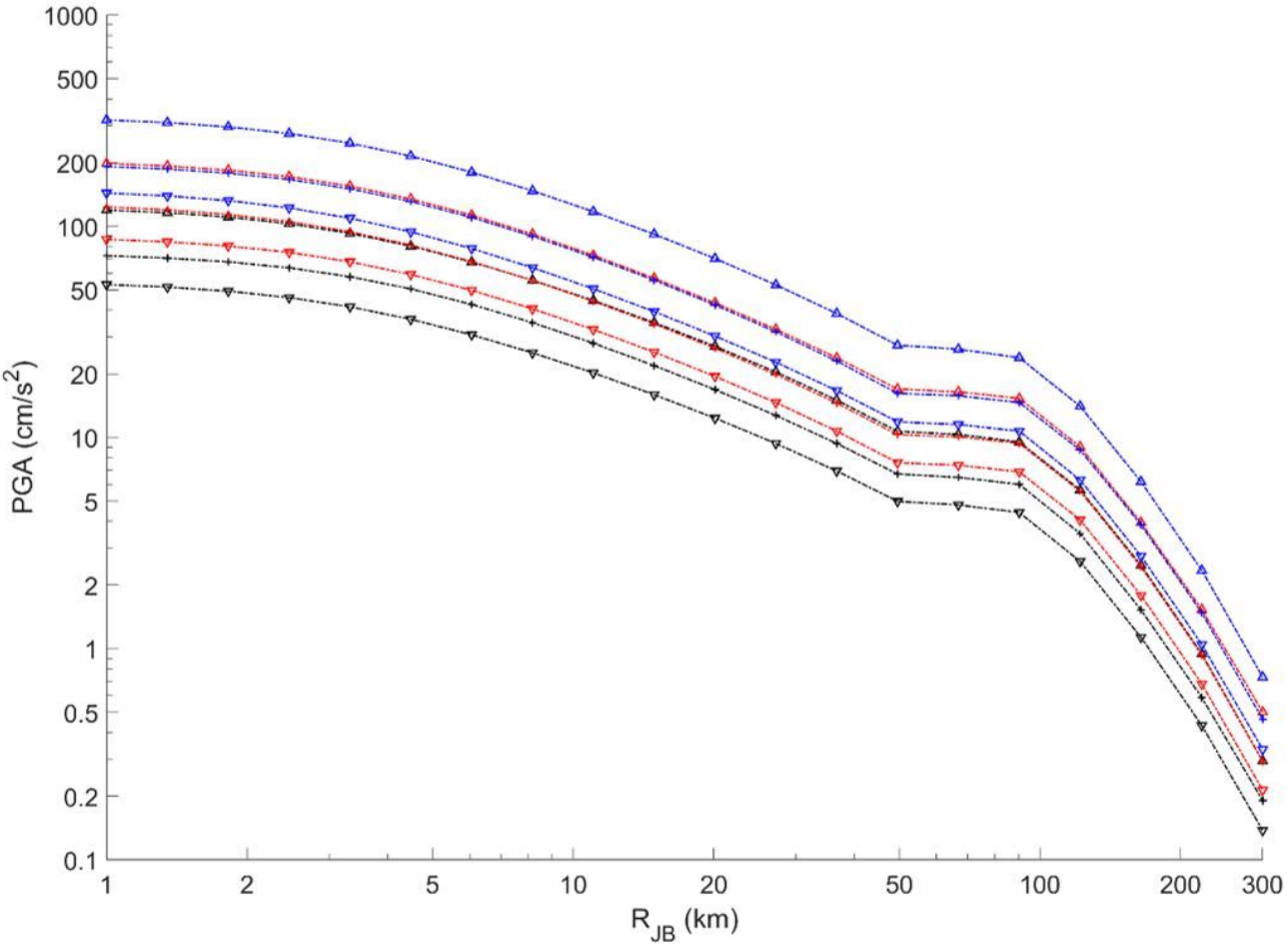

Figure 2

Ground-motion models derived for the SZC site using the HEM for PGA and magnitude 5 against R_{JB}, distance to the surface projection of rupture. The blue curves are for 20 MPa, red for 10 MPa, black for 5 MPa, the upward triangles are for kappa=0.01 s, the crosses for kappa=0.02 s and the downward triangles for kappa=0.03 s.

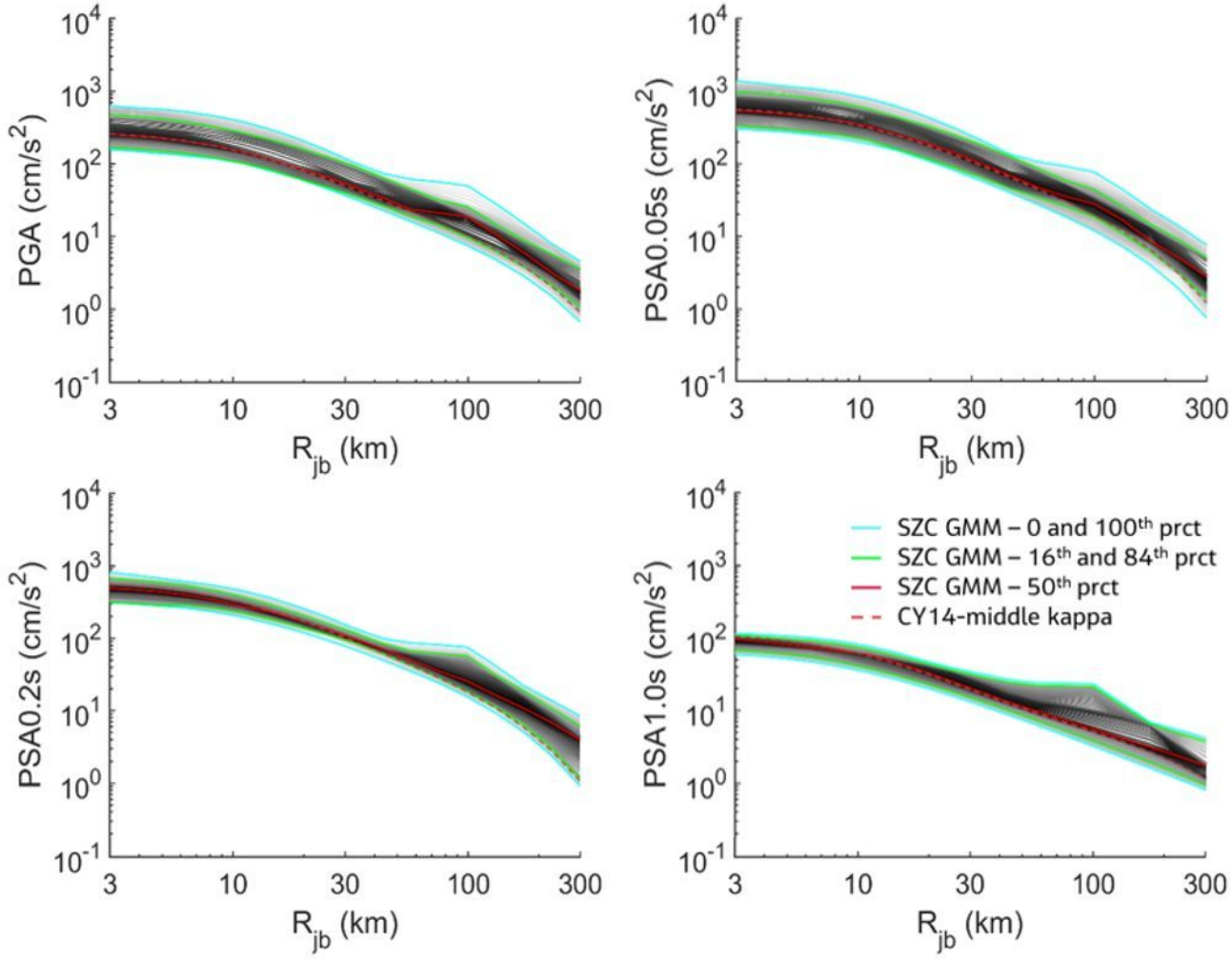

Figure 3

Distance scaling for PGA and PSA at 0.05, 0.2 and 1.0 s for magnitude M 6.0 at percentiles between 0 and 100, in steps of 1 percent, for the SZC GMM predictions (grey lines; cyan, green and read lines show selected percentiles) and the median prediction of CY14-middle kappa (red dashed line).

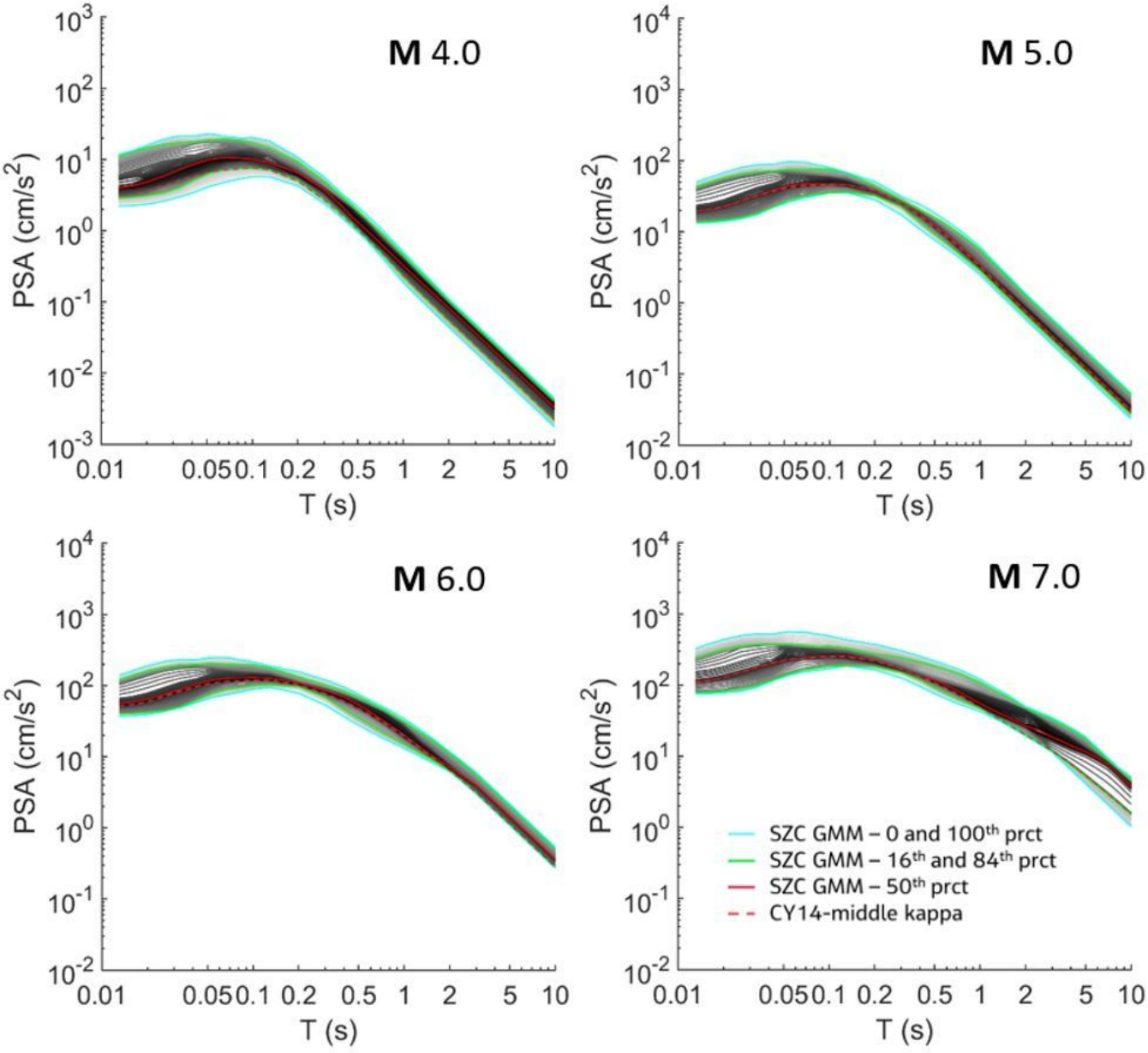

Figure 4

Response spectra for M 4.0, 5.0, 6.0 and 7.0 at 30 km at percentiles between 0 and 100, in steps of 1 percent, for the SZC GMM predictions (grey lines; cyan, green and read lines show selected percentiles) and the median prediction of the CY14-middle kappa (red dashed line).

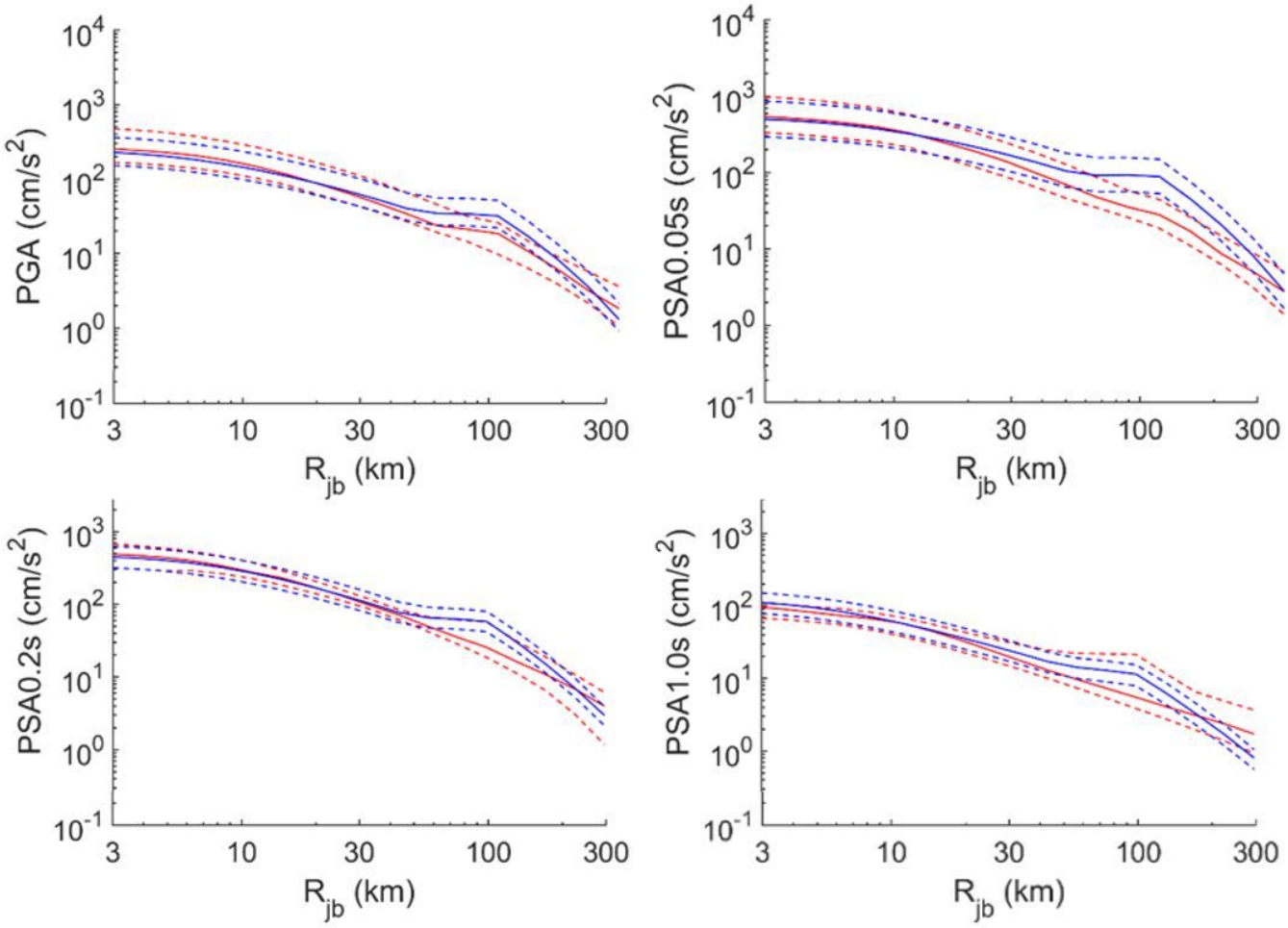

Figure 5

Distance scaling plots for PGA and PSA at 0.05, 0.2 and 1.0 s for the 16th, 50th and 84th percentile predictions of the SZC GMM (red lines) and UK backbone (blue lines) models.

Dashed lines show the 16th and 84th percentiles; solid lines correspond to the 50th percentile.

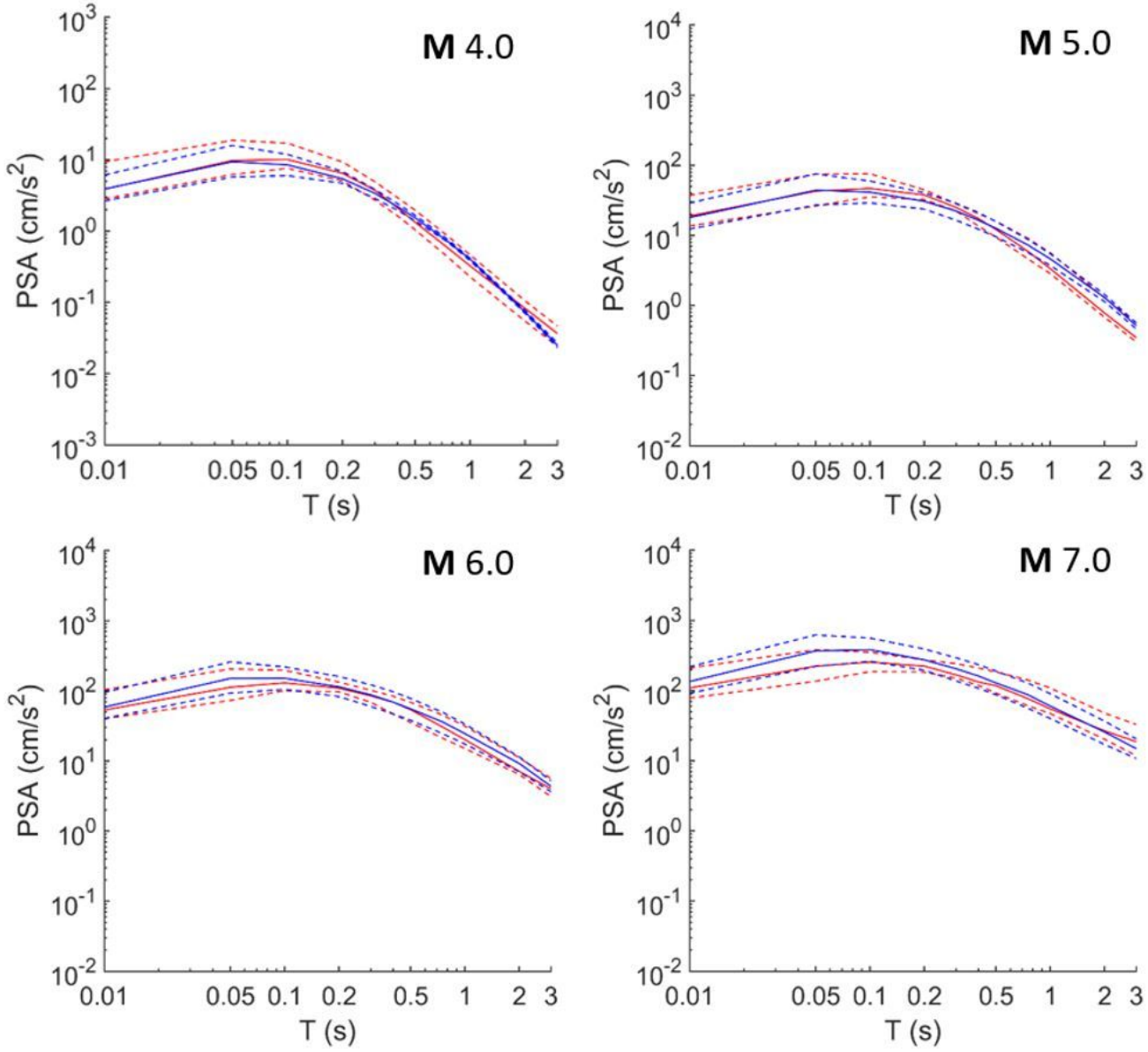

Figure 6

Response spectra for the 16th, 50th and 84th percentiles of the SZC GMM (red lines) and UK backbone (blue lines) models for magnitudes M 4.0, 5.0, 6.0 and 7.0.

Dashed lines show the 16th and 84th percentiles; solid lines correspond to the 50th percentile.

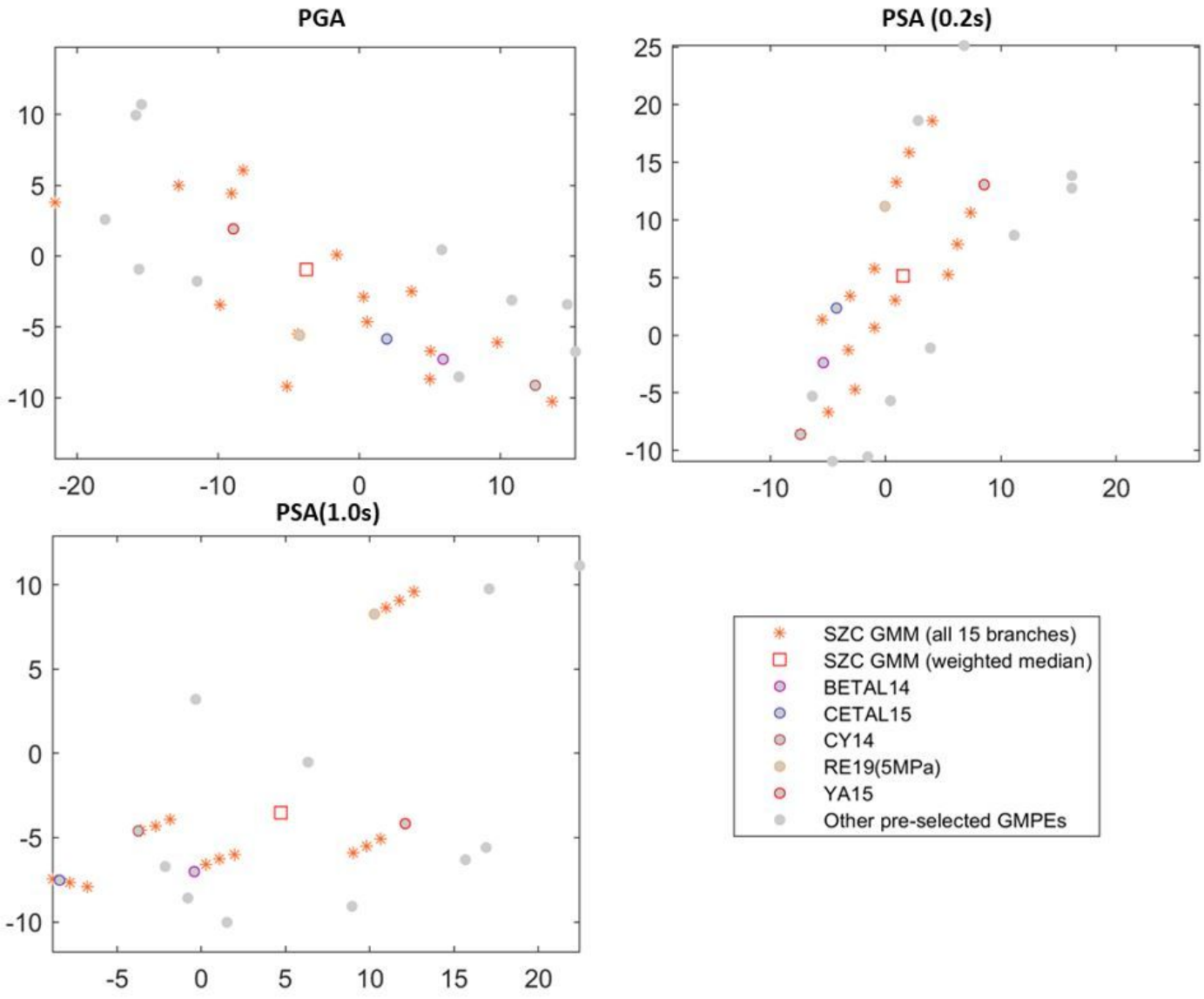

Figure 7

Sammon's maps for PGA and PSA at 0.2 and 1.0 s considering all preliminary selected GMPEs.

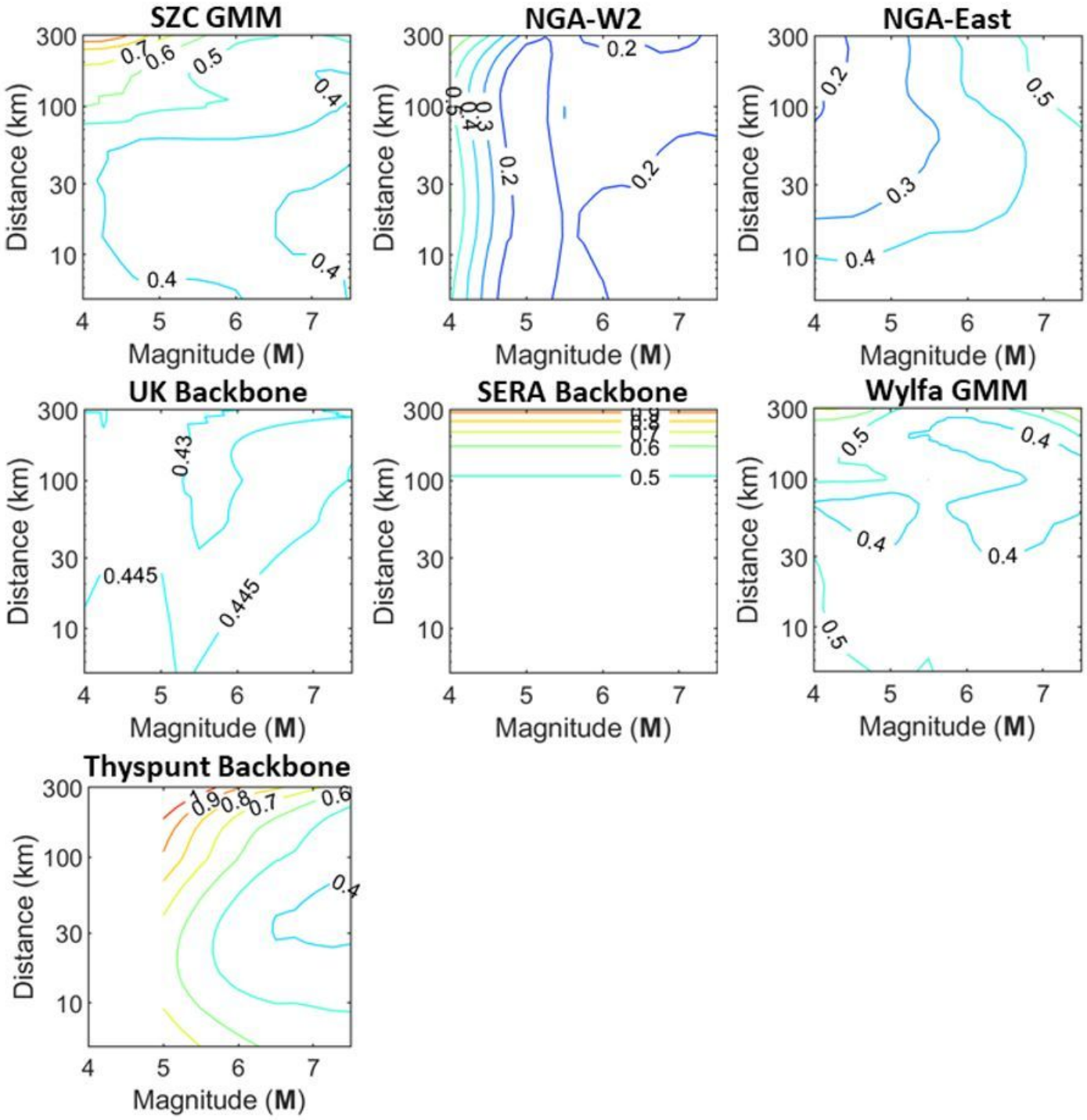

Figure 8

Comparison of σ_{μ} for PGA for the selected GMMs.

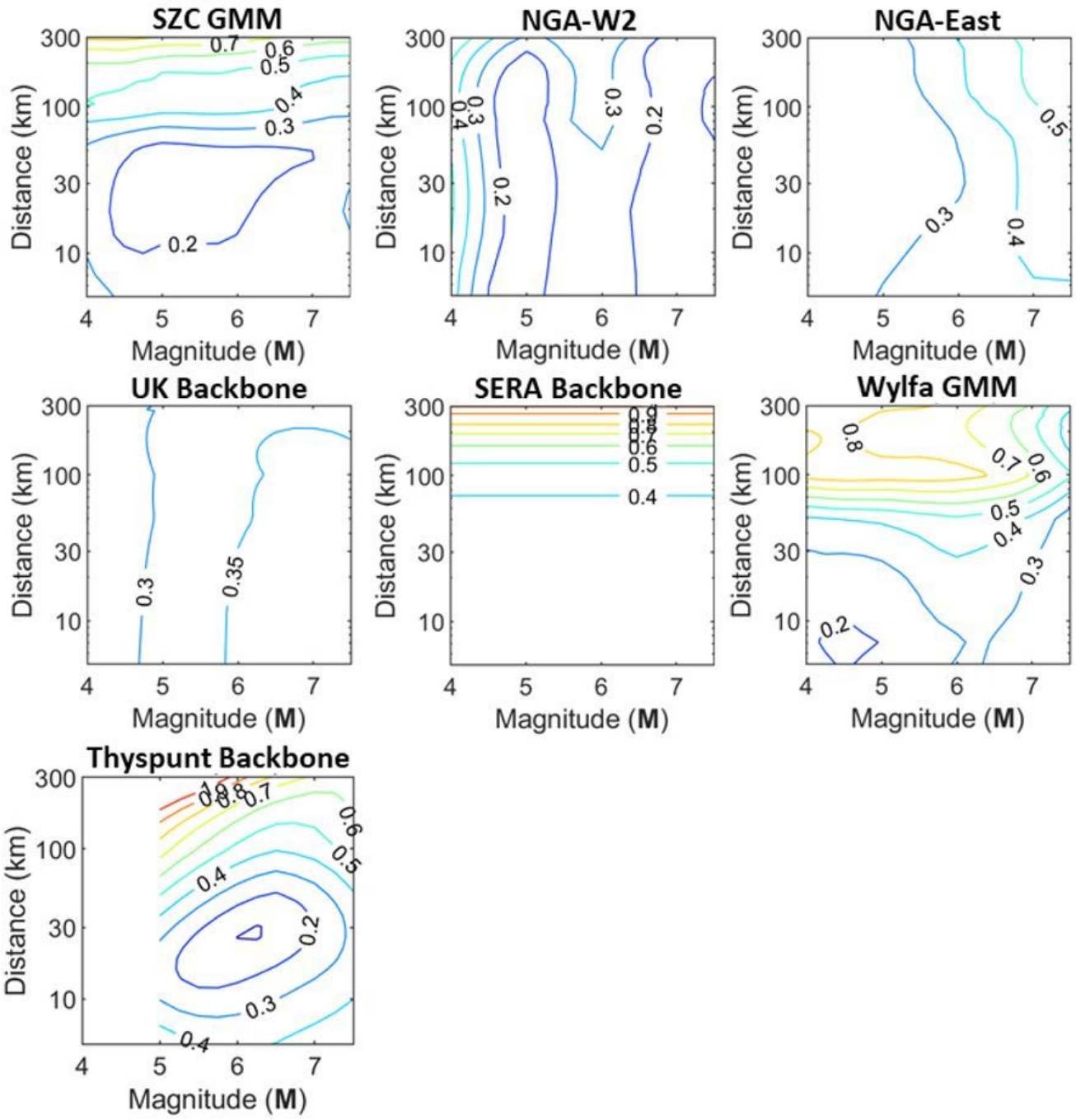

Figure 9

Comparison of σ_μ for PSA at 0.2 s for the selected GMMs.

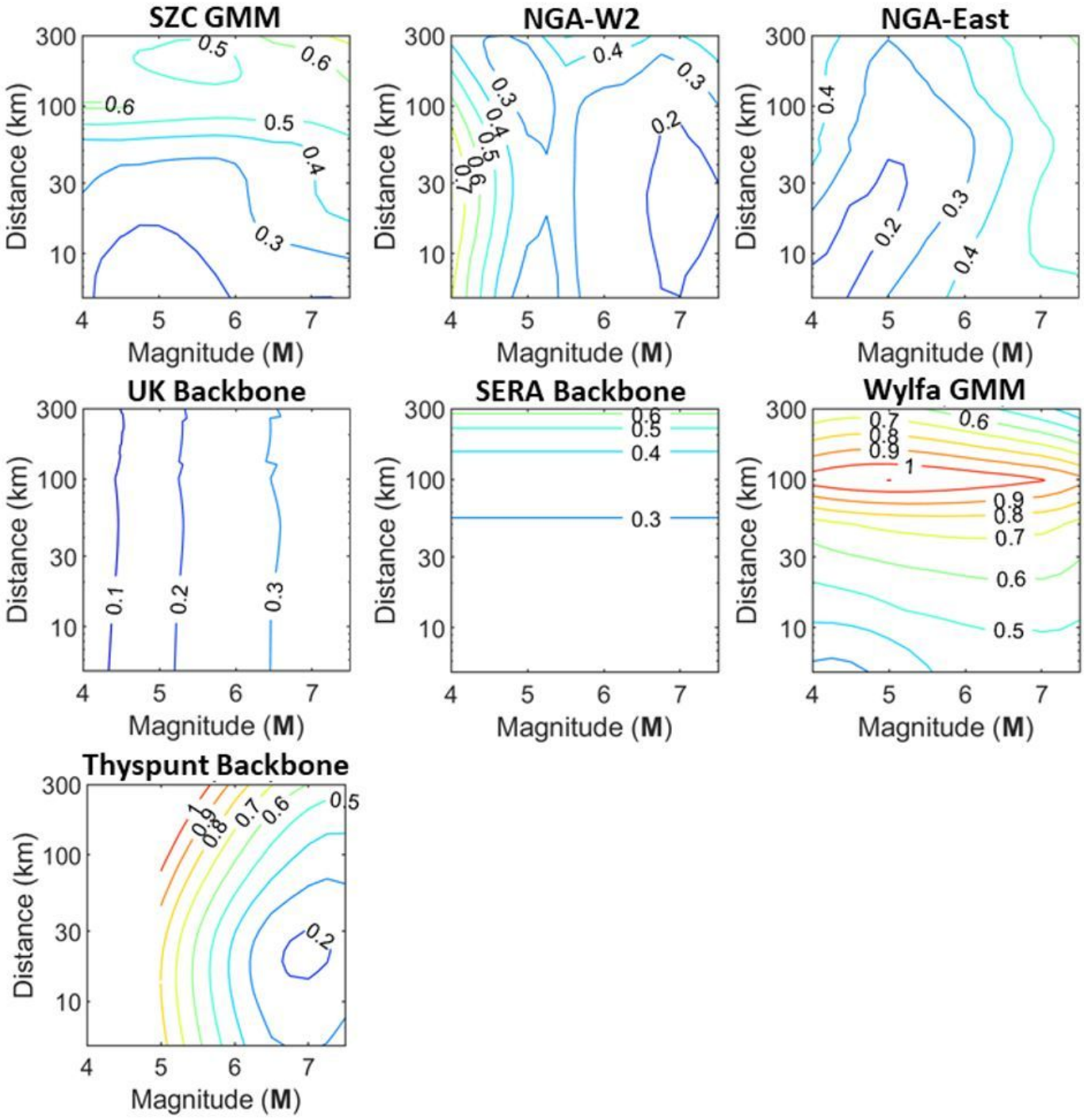

Figure 10

Comparison of σ_μ for PSA at 1.0 s for the selected GMMs.

Figure 11

σ_μ estimates at the reference velocity horizon from the final hazard calculations for the SZC site.